THE JOURNAL OF BIOLOGICAL CHEMISTRY
Vol. 279, No. 3, Issue of January 16, pp. 1968–1979, 2004
Printed in U.S.A.

Molecular Cloning, Genomic Structure, and Expression Analysis of MUC20, a Novel Mucin Protein, Up-regulated in Injured Kidney*[S]

Received for publication, May 1, 2003, and in revised form, October 17, 2003
Published, JBC Papers in Press, November 5, 2003, DOI 10.1074/jbc.M304558200

Toshio Higuchi‡§, Takuya Orita‡§, Setsuko Nakanishi‡, Ken Katsuya‡, Hirotaka Watanabe‡, Yoshiki Yamasaki‡, Iwao Waga‡, Toyomichi Nanayama¶, Yoshihisa Yamamoto¶, William Munger‖, Hong-Wei Sun‖, Ronald J. Falk, J. Charles Jennette**, David A. Alcorta**, Huiping Li‡‡, Tadashi Yamamoto‡‡, Yutaka Saito‡, and Motonao Nakamura‡§§**

*From the ‡Central Pharmaceutical Research Institute, Pharmaceutical Frontier Research Laboratories, Japan Tobacco Inc., Yokohama, Kanagawa, 236-0004, Japan, ¶Central Pharmaceutical Research Institute, Japan Tobacco Inc., Takatsuki, Oosaka, 569-1125, Japan, ‖Gene Logic Inc., Gaithersburg, Maryland 20878, **Division of Nephrology and Hypertension, Department of Medicine, University of North Carolina, Chapel Hill, NC 27599-7155, and the ‡‡Institute of Nephrology, Faculty of Medicine Niigata University, Niigata, 951-8510, Japan*

Immunoglobulin A nephropathy (IgAN) is the most common primary glomerulonephritis in the world. Here, we identify a cDNA encoding a novel mucin protein, shown previously to be up-regulated in IgAN patients, from a human kidney cDNA library. This protein contains a mucin tandem repeat of 19 amino acids consisting of many threonine, serine, and proline residues and likely to be extensively *O*-glycosylated; thus, this gene was classified in the mucin family and named MUC20. The human *MUC20* gene contains at least four exons and is localized close to *MUC4* on chromosome 3q29. We found variations in repeat numbers in the mucin tandem domain, suggesting polymorphism of this region. Northern blot and reverse transcription-PCR analyses revealed that human MUC20 mRNA was expressed most highly in kidney and moderately in placenta, colon, lung, prostate, and liver. Immunohistochemical analysis of human kidney revealed that MUC20 protein was localized in the proximal tubules. Immunoblotting analysis of MUC20 proteins produced in Madin-Darby canine kidney and HEK293 cells indicated the localization of MUC20 protein in a membrane fraction and extensive posttranslational modification. Immunoelectron microscopy of MUC20-producing Madin-Darby canine kidney cells demonstrated that MUC20 protein was localized on the plasma membrane. Expression of MUC20 mRNA in a human kidney cell line was up-regulated by tumor necrosis factor-α, phorbol 12-myristate 13-acetate, or lipopolysaccharide. Two species of MUC20 mRNA (hMUC20-L and hMUC20-S), resulting from alternative transcription, were identified in human tissue, whereas only one variant was observed in mouse tissues. Mouse MUC20 mRNA was expressed in the epithelial cells of proximal tubules, and the expression increased dramatically with the progression of lupus nephritis in the kidney of MRL/MpJ-*lpr/lpr* mice. Moreover, the expression of mouse MUC20 was augmented in renal tissues acutely injured by cisplatin or unilateral ureteral obstruction. These characteristics suggest that the production of MUC20 is correlated with development and progression of IgAN and other renal injuries.

Epithelial cell injury in renal tissue is a feature of many acute and chronic kidney diseases. Among the morphological changes observed are loss of the proximal tubular brush border, loss of cellular polarity, and dedifferentiation and apoptosis of the proximal tubule epithelial cells. During progression of renal injury, necrotic tubular epithelial cells detach from the basement membrane and cause intraluminal obstruction. After surviving dedifferentiated cells spread over the denuded basement membrane, functional epithelia are reformed by the dedifferentiated cells undergoing mitogenesis, redifferentiation, and re-establishment of normal epithelial polarity (1, 2). Although these processes are well described at the histological level, very little is known about the molecular levels involved. To date, some mucin proteins, such as MUC1, MUC3, and kidney injury molecule-1 (KIM-1), have been identified as proteins likely to regulate these renal events. MUC1 mRNA is expressed in the distal convoluted tubules and collecting ducts; MUC3 mRNA is in the proximal tubules and is overexpressed in renal cell carcinoma patients (3). KIM-1 mRNA is drastically up-regulated in the epithelial cells of the regenerating proximal tubules following ischemia (4).

In general, mucins are divided into two structurally and functionally distinct classes, the secreted and the transmembrane types. Human MUC2, MUC5A, MUC5B, MUC6, MUC7, MUC8, and MUC9 are classified as secreted types (5–11), whereas MUC1, MUC3, MUC4, MUC12, MUC13, MUC15, MUC16, MUC17, MUC18, and KIM-1 are transmembrane types (4, 12–21). Some of the mucin genes are clustered in the human genome, *e.g. MUC2*, *MUC5A*, *MUC5B*, and *MUC6* genes are located on chromosome 11p15.5 (22), and *MUC3A*, *MUC3B*, *MUC11*, *MUC12*, and *MUC17* genes are on chromosome 7q22 (14, 16, 20).

Recently, we have identified several cDNA fragments with altered expression in renal tissues of patients with immunoglobulin A nephropathy (IgAN),[1] using the Gene Logic propri-

* The costs of publication of this article were defrayed in part by the payment of page charges. This article must therefore be hereby marked "*advertisement*" in accordance with 18 U.S.C. Section 1734 solely to indicate this fact.

The nucleotide sequence(s) reported in this paper has been submitted to the GenBank™/EBI Data Bank with accession number(s) AB098731, AB098733, AB098732

[S] The on-line version of this article (available at http://www.jbc.org) contains supplementary figure showing the location of the MUC20 protein in the proximal tubules.

§ Both authors contributed equally to this work.

§§ To whom correspondence should be addressed. Tel.: 81-45-786-7693; Fax: 81-45-786-7692; E-mail: motonao.nakamura@ims.jti.co.jp.

[1] The abbreviations used are: IgAN, immunoglobulin A nephropathy; BUN, blood urea nitrogen; DIG, digoxigenin; Dox, doxycycline; EST,

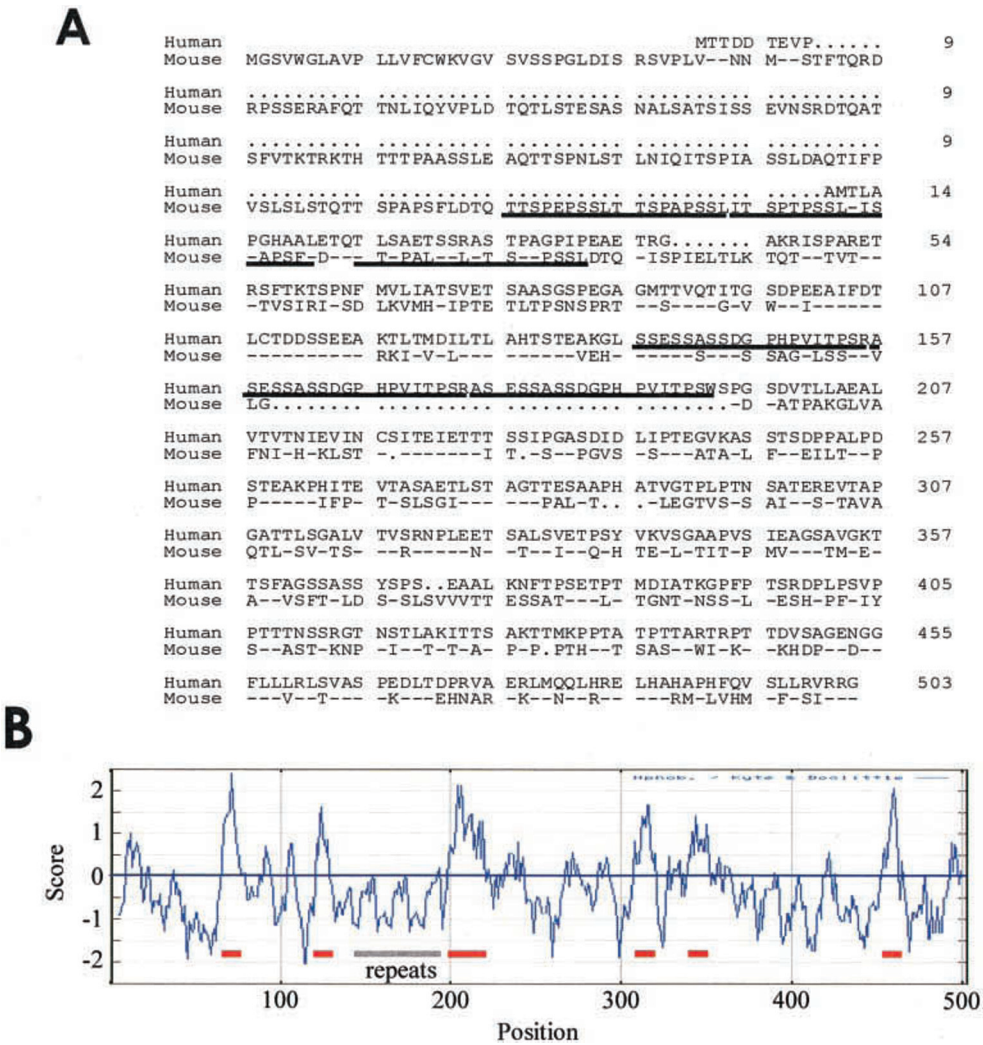

FIG. 1. **Comparison of the deduced amino acid sequences of human and mouse MUC20.** In *A*, identical amino acids of mouse MUC20 and human MUC20 are shown by *dashes*. *Periods* represent spaces added for proper alignment. The mucin repeat regions of human and mouse MUC20 are *underlined*. *B*, hydropathy profile of human MUC20, calculated according to the Kyte-Doolittle algorithm. The mucin repeat region is indicated by a *gray bar*, and the hydrophobic domains are indicated by *red bars*.

etary READS® mRNA differential display technology (23, 24). Probing a human kidney cDNA library with one of these fragments, EST22972 (24), we obtained a human cDNA encoding a novel mucin membrane protein, MUC20. Here we describe the molecular cloning, genomic structure, and expression analysis of MUC20 in human normal tissues as well as in animal models of renal injury.

MATERIALS AND METHODS

Cloning of the Human MUC20 cDNA and Its Genomic DNAs—A full-length cDNA encoding human MUC20 was obtained by an oligonucleotide-pulling method. Briefly, a gene-specific oligonucleotide was designed based on the sequence of the EST22972 fragment identified as described previously (24) and labeled with biotin. The biotin-labeled oligonucleotide was used for hybridization with single-stranded plasmid DNAs derived from a human kidney cDNA library (Origene) following the procedures of Sambrook *et al.* (25). The hybridized cDNAs were separated by streptavidin-conjugated beads and then eluted by heating. After the eluted cDNAs were converted to double-stranded plasmid DNAs, the longest cDNA was sequenced. A human genomic DNA library (λFIX II) was purchased from Stratagene and screened (1.0×10^6 plaques) with the human MUC20 cDNA labeled with [α-^{32}P]dCTP (Amersham Biosciences) by random priming. Hybridization was performed as described previously (26). The human *MUC20* gene-bearing plasmids were converted from the isolated phage DNAs purified from positive plaques and subjected to restriction mapping and DNA sequencing.

Cloning of the Mouse MUC20 cDNA—Searching the mouse EST data base yielded two EST fragments, BF119189 and BE689844, with high identities to human MUC20. We then isolated and sequenced the mouse cognate from a mouse kidney cDNA library (Takara) by PCR screening based on the sequences of these ESTs.

RACE PCR—RACE PCR of the 5′-terminus of MUC20 mRNA was carried out using a SMART™ RACE cDNA amplification kit (Clontech) following the manufacturer's protocol. For analysis of human MUC20 mRNA, the primary PCR amplification was performed using the oligonucleotide 5′-CTTCTGTGGAGGTGTGAGCCAATGT-3′ as a gene-specific primer and total RNA from the human kidney (Clontech) as a template. Secondary PCR amplifications were conducted using oligonucleotides 5′-CCTGTGATGGTCTGAACTGTGGTCA-3′, 5′-CTCCCCTGGTCTCTGCTTCTGGAAT-3′, and 5′-CACTTCTGTGTCGTCCGTTGTCATC-3′ as gene-specific primers A–C, respectively. For the analysis of the mouse MUC20 mRNA, the primary PCR amplification was carried out using the oligonucleotide 5′-CAGTTCTGGGGCTGTTGCTTGGTGTCA-3′ as a gene-specific primer and total RNA prepared from kidney as a template. The secondary PCR amplifications were conducted by using oligonucleotides 5′-AGGGTCAATTCAATAGGCGAGATGGTC-3′, 5′-GGGTATCCAGGAATGACGGTGCAGGGG-3′, and 5′-ATGGT-

expressed sequence tag; GAPDH, glyceraldehyde-3-phosphate dehydrogenase; IL, interleukin; MDCK, Madin-Darby canine kidney; RACE, rapid amplification of cDNA ends; RT, reverse transcription; UUO, unilateral ureteral obstruction; PBS, phosphate-buffered saline; ERK, extracellular signal-regulated kinase; NCBI, National Center for Biotechnology Information; h, human; m, mouse.

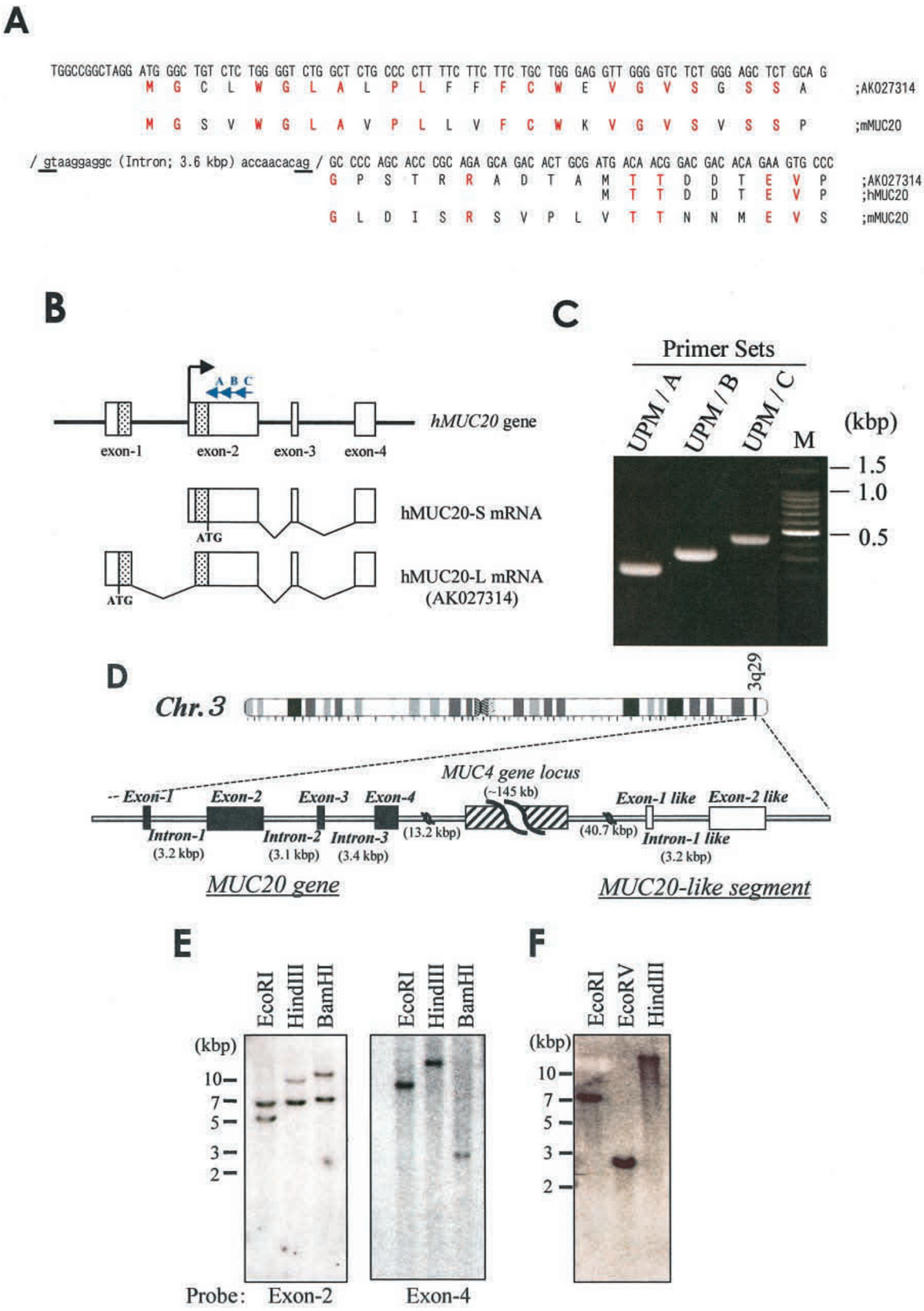

FIG. 2. **Genomic structure of the human *MUC20* gene.** *A*, the nucleotide and amino acid sequences of the N terminus of the AK027314 clone, including the exon/intron boundary sequence. The deduced amino acid sequences of the isolated human MUC20 (hMUC20) and mouse MUC20 (mMUC20) are also shown. The nucleotide sequences of the exons and intron are represented as *capital* and *lowercase letters*, respectively. The predicted splicing sites in the intron are *underlined*. Amino acids identical among the AK027314 clone, the isolated human, and the mouse MUC20 are shown in *red*. *B*, exon maps of the hMUC20-L and hMUC20-S mRNAs, as determined by sequencing of the genomic and cDNA clones. The exons are indicated as *open boxes*, and the domains encoding the additional 35 amino acids found in hMUC20-L are indicated as *dotted boxes*. The reverse PCR primers, primers A–C, used for the RACE analysis described in *C* are shown by *blue arrows*. Locations of the start codon in each mRNA are indicated as *ATG*. The transcriptional start point of hMUC20-S determined by 5′-RACE is indicated by a *black arrow*. *C*, RACE PCR analysis of the 5′-terminus of MUC20 mRNA expressed in human kidney. These experiments used primers A–C depicted in *B* and Universal Primer Mix™ (UPM™) (Clontech) (*UPM*) primer. Primer sets used in each reaction are indicated *above* the *lanes*. Molecular sizes (kbp) are shown on the *right*.

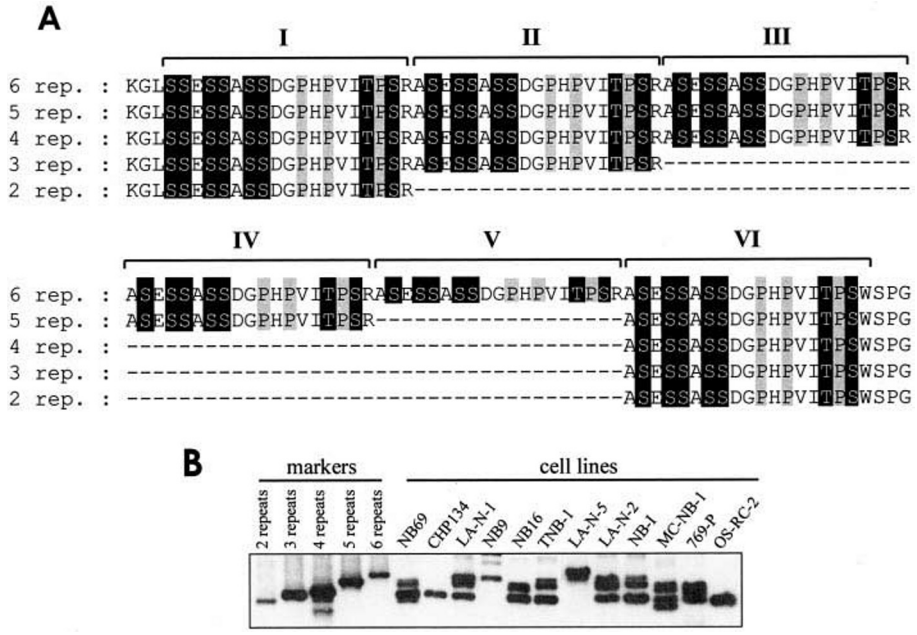

FIG. 3. **Polymorphism of the human MUC20 tandem domain.** *A*, amino acid sequence alignment of the tandem domains (2-, 3-, 4-, 5-, and 6-repeat (*rep.*) forms) in cloned human MUC20. Repeat numbers of the longest form are represented as *I–VI*, and other types are aligned to this form. All threonine and serine residues in the domains are indicated by *reversed type*, and proline residues are indicated by *gray shading*. *Dashes* represent spaces added for proper alignment. *B*, the repeat numbers of the tandem domain in the human *MUC20* gene from several human cell lines. Determination of the tandem domain size was performed by PCR amplification of these domains followed by Southern blot analysis. The standard sizes of 2–6 repeats of the tandem domain are shown as *markers*. Since the primers were able to amplify the tandem domain in the *MUC20-like* segment as well as that in the *MUC20* gene, 1–4 species were generated in each cell line.

TCAGGGGAAGTGGTTTGGGTAT-3′ as gene-specific primers A–C, respectively.

Southern Blot Analysis of Genomic DNA—Human and mouse genomic DNAs (Clontech) were digested with various restriction enzymes. The digested fragments were separated by electrophoresis on a 0.8% agarose gel, transferred onto a nylon membrane (Hybond-N^+, Amersham Biosciences), and then hybridized at 65 °C with an [α-^{32}P]-labeled probe described below. For the human blot hybridization, two probe fragments, the *exon-2* and the *exon-4* segments, were prepared by PCR using primer sets 5′-TGAAGAGGCAAAGACACTCACAATG-3′ and 5′-CTGTTGGGGGCTTCATCGTGGTCTT-3′ for the *exon-2* probe and 5′-AACTCCACGCCCACGCGCCT-3′ and 5′-GGAAGCACACAGATGGGTGA-3′ for the *exon-4* probe, with the human MUC20 cDNA as a template. For the mouse blotting analysis, the probe fragment corresponding to the *exon-2* segment was prepared by PCR using the primer set, 5′-ATGGAAGTGTCCACCTTCACTC-3′, and 5′-TGTGCCAGTTTGGACAGTGC-3′, with the mouse MUC20 cDNA as a template. PCR was carried out for 35 cycles of denaturation at 94 °C for 0.5 min, annealing at 55 °C for 0.5 min, and extension at 72 °C for 1 min using a model 9600 thermal cycler (PerkinElmer Life Sciences).

Analysis of the Polymorphic Region of Human MUC20—Cell lines used in these experiments were purchased from the following sources: human neuroblastoma cell lines, NB69, CHP134, LA-N-1, NB9, NB16, TNB-1, LA-N-5, LA-N-2, NB-I, and MC-NB-1 were purchased from Riken Gene Bank, and human kidney cell lines, 769-P, and OS-RC-2 were purchased from the American Type Culture Collection (ATCC), and cell lines were grown as recommended by the suppliers. Genomic DNAs were prepared from these cell lines as described (27). To estimate repeat numbers, the tandem domains in the human *MUC20* gene derived from these cell lines were amplified by PCR using the specific primer set 5′-CCCTTTGCACCGATGACAG-3′ and 5′-TTCCAGGGGATTCCTGCT-3′ under the thermal cycling conditions described above. The PCR-amplified fragments were separated by electrophoresis on a 1.5% agarose gel, transferred onto a nylon membrane (Hybond-N^+, Amersham Biosciences), and then detected by Southern blot analysis using a fluorescein-labeled oligonucleotide (5′-CACACCTCCACAGAAGCTAAG-3′), complementary to the repeat region of MUC20, as a probe.

Northern Blot Analysis—Multiple tissue Northern blots of human and mouse tissues were purchased from Clontech and hybridized with the [α-^{32}P]-labeled human *exon-2*, human *exon-4*, or mouse *exon-2* DNAs prepared as described above. Hybridization was performed as described previously (26). The resulting filters were autoradiographed with a BAS2000 system (Fuji Film).

RT-PCR—Poly(A)+ RNAs from human brain, heart, kidney, liver, lung, pancreas, placenta, and skeletal muscle were purchased from Clontech. Human kidney cell lines ACHN, OS-RC-2, 769-P, TUHR-4-TKB, and A704 were purchased from ATCC and grown as recommended for each cell line. ACHN cells were stimulated with transforming growth factor-β (2 ng/ml; Peprotech), phorbol 12-myristate 13-acetate (100 μM; Sigma), lipopolysaccharide (10 μg/ml; Sigma), IL-1β (0.4 ng/ml; Peprotech), IL-6 (100 ng/ml; Peprotech), IL-8 (250 ng/ml; Peprotech), or tumor necrosis factor-α (100 ng/ml; Peprotech) for 14 h. Total RNA was isolated with TRIzol reagent (Invitrogen). Reverse transcription was carried out using an Advantage™ RT-for-PCR kit (Clontech) following the manufacturer's protocol. PCR was performed under the thermal cycling conditions described above. The primer sets were as follows: for human MUC20 mRNA, 5′-AACTCCACGCCCACGCGCCT-3′ and 5′-GGAAGCACACAGATGGGTGA-3′, and for mouse MUC20 mRNA, 5′-ACCCTTTGTACCGATGACAGCTCTGAAGAG-3′ and 5′-CAAGCAGTGGATGCAGATGTTGTAGGATG-3′. The primers used for GAPDH mRNA detection were purchased from Clontech.

Quantitative RT-PCR—Total RNA was reverse-transcribed using TaqMan reverse transcription reagents (Applied Biosystems). PCR was performed using probes with SYBER Green (Molecular Probes) on an ABI PRISM 7000 sequence detection system (Applied Biosystems). The primer pairs used for the PCR amplification were as follows: for mouse MUC20 mRNA, 5′-CGTGGCCTCCCCTAAGGA-3′ and 5′-ATGCGGGCGTGCAGTT-3′, and for mouse collagen type I mRNA, 5′-AGAGCATGACCGATGGATTCC-3′ and 5′-TTGCCAGTCTGCTGGTCCATG-3′. The primers used for GAPDH mRNA were purchased from Clontech.

Cells and Transfections—The pBI-MUC20 plasmid was constructed

M, molecular size maker. *D*, chromosomal localization and exon mapping of the human *MUC20* gene, as determined by sequencing of the genomic DNAs and cDNA clones, are shown. Human chromosome 3 is shown schematically. Exons on the human *MUC20* gene locus are indicated as *closed boxes*. The *MUC20-like* segment (*open boxes*) and the *MUC4* gene (*striped box*) are also indicated. *E* and *F*, Southern blot analyses of human (*E*) and mouse (*F*) *MUC20* genes. Genomic DNAs were digested with the indicated restriction enzymes. Probes corresponded to a part of the *exon-2* (*E*, *left panel*) or *exon-4* (*E*, *right panel*) in the human gene or the *exon-2* fragment in the mouse gene (*F*).

by cloning of a C-terminally FLAG-tagged human MUC20 cDNA prepared by PCR into the pBI-L vector (Clontech). All materials for a Tet-Off system, including human embryonic kidney 293 (HEK293) and Madin-Darby canine kidney (MDCK) Tet-Off cells, were purchased from Clontech. The cells were grown in the presence of 2 μg/ml doxycycline (Dox) as recommended. For generation of the cell lines stably expressing the FLAG-tagged human MUC20, both pBI-MUC20 and pTK-Hyg plasmids (ratio 10:1) were co-transfected into Tet-Off MDCK or Tet-Off HEK293 cells using GeneJammer reagent (Stratagene) as described in the manufacturer's procedure, and then hygromycin-resistant clones were selected. Hygromycin-resistant clonal lines were established by limiting dilution, and the production of MUC20 protein in each line was confirmed by immunoblotting analysis with an anti-FLAG (M2) antibody (Sigma).

Immunoblotting—A rabbit polyclonal antibody, anti-MUC20, was raised against the N-terminal domain of human MUC20 using a synthetic peptide, RGAKRISPARETRSFTK (residues 46–62), coupled to keyhole limpet hemocyanin. For immunoblotting, cells were suspended in lysis buffer (1% Nonidet P-40, 137 mM NaCl, 10% glycerol, 1 mM Na_3VO_4, and 20 mM Tris-HCl, pH 8.0) containing protease inhibitors (1 mM phenylmethylsulfonyl fluoride, 0.2 trypsin inhibitory units/ml aprotinin, and 20 μg/ml leupeptin). The resulting lysates were centrifuged to remove cellular debris, and then the postnuclear supernatants were centrifuged at 100,000 $\times$ *g* to separate the membrane pellet fractions and the cytosolic supernatants. Protein concentrations were determined using Bio-Rad protein assay reagent. Proteins (5 μg) were analyzed by immunoblotting with primary antibodies and horseradish peroxidase-conjugated secondary antibodies, and specific bands were detected with the ECL system (Amersham Biosciences).

Immunocytochemistry—MDCK/*tet*-MUC20 cells were washed in phosphate-buffered saline (PBS) and fixed with 4% paraformaldehyde with 0.1% glutaraldehyde in 0.1 M phosphate buffer, pH 7.4, for 30 min. After blocking with Tris-glycine and an endogenous biotin blocking kit (DAKO), the cells were further blocked with antibody diluent containing 2% goat normal serum and 0.1 mg/ml bovine serum albumin. The cells were incubated with polyclonal antibody against human MUC20 or rabbit IgG at 1 μg/ml. The cells were washed and incubated with biotinylated $F(ab')_2$ fragments of anti-rabbit IgG (Cappel) at 5 μg/ml. Visualization was done with labeled streptavidin-boitin system (labeled streptavidin biotin kit, DAKO). The cells were postfixed with 1% osmium tetroxide in 0.1 M cacodylate buffer, pH 7.4, and embedded in Epon. Ultrathin sections were examined with a Hitachi H-7100 electron microscope at 75 kV without counterstaining.

Animals—Female MRL/MpJ-*lpr/lpr* mice (SLC Japan) were sacrificed under anesthesia at different ages (1–9 months), and blood urea nitrogen (BUN) was measured using an autoanalyzer (COBAS FARA; Roche Applied Science). Acute renal injury was induced in Charles River CD-1 mice (male, 6 weeks old, Charles River, Japan) by subcutaneous administration of cisplatin (18 mg/kg; Nippon Kayaku), and both serum creatinine and BUN were measured to evaluate renal damage using the autoanalyzer. Unilateral ureteral obstruction (UUO) was induced in C57Bl(B6) mice (male, 8 weeks old, Charles River, Japan) as described (28). Collagen type I mRNA in the kidney was measured by quantitative RT-PCR, and the content of hydroxyproline was quantified as described (29).

In Situ Hybridization—Two fragments (fragment 5-1, 747 bp, and fragment 7-11, 892 bp) were prepared from mouse MUC20 cDNA by PCR, using the following primer sets: 5′-ATGGAAGTGTCCACCTTCACTC-3′ and 5′-TGTGCCAGTTTGGACAGTGC-3′ for fragment 5-1, and 5′-AGCACCTGTCTTCAGAGAGC-3′ and 5′-TGCTCAGTGAGGTCCTTAGG-3′ for fragment 7-11, with the mouse MUC20 cDNA as a template. As a positive control, a fragment of mouse TSC-22 was also synthesized by PCR using specific primers 5′-AAGTGGAAGTTCTGAAGGAGC-3′ and 5′-TAAGATAGCCTAGGTCCCAGC-3′, with the mouse TSC-22 cDNA as a template. After subcloning the PCR products into the pGEN-T vector (Promega) followed by linearization of each plasmid with appropriate restriction enzymes, digoxigenin (DIG)-labeled single-stranded antisense and sense probes were generated using T7 and Sp6 RNA polymerases (Roche Applied Science), respectively, using a DIG RNA labeling kit (Roche Applied Science).

Five-, 9-, 23-, and 60-week-old MRL/MpJ-*lpr/lpr* mice and 23-week-old C57Bl(B6) mice were anesthetized with ethyl ether and fixed by cardiac perfusion with 4% paraformaldehyde in 0.1 M phosphate buffer, pH 7.4. Dissected kidneys were further fixed in the same fixative overnight at 4 °C. Cryosections of 10 μm were dried at 45 °C for 2 h and rinsed three times with PBS for 5 min each followed by one rinse with distilled water for 5 min. After incubation in 0.2 N HCl for 20 min and then in a 10 μg/ml proteinase K solution for 20 min, the sections were rinsed with PBS and fixed in 4% paraformaldehyde in 0.1 M phosphate buffer, pH 7.4, for 5 min. After equilibration with glycine in PBS twice for 15 min each, the sections were dehydrated with graded alcohol and air-dried for 10 min. DIG-labeled cRNA probes were denatured at 85 °C for 5 min. The resulting sections were incubated with probe at 50 °C overnight, washed with 2× SSC at 50 °C twice for 15 min each and at 55 °C for 1 h, followed by a 1-h wash with 0.2× SSC at 55 °C. Immunohistochemical detection of DIG using an alkaline phosphatase-labeled antibody was performed as recommended by Roche Applied Science (30). After stopping the reaction, sections were fixed with 4% paraformaldehyde in 0.1 M phosphate buffer, pH 7.4, for 1 h and counterstained with methyl green.

RESULTS

Cloning of Human and Mouse MUC20 cDNAs—EST22972 is a gene fragment whose expression was shown to be up-regulated in renal tissues of IgAN patients (24). To isolate the full-length cDNA corresponding to the EST22972 fragment, we screened a human kidney cDNA library with an oligonucleotide probe based on the sequence of EST22972. A clone was isolated, and sequence analysis revealed an open reading frame encoding 503 amino acids with several hydrophobic domains, suggesting that this protein is a membrane protein (Fig. 1, *A* and *B*). In addition, this protein has 3 tandem repeats of 19 amino acids mainly consisting of threonine, serine, and proline residues likely to be extensively *O*-glycosylated (Fig. 1*A*). Because of the similarity of this tandem domain to sequences conserved among mucins, we named this clone MUC20.

A BLAST search (31) of the mouse data base at the National Center for Biotechnology Information (NCBI) revealed that mouse ESTs BF119189 and BE689844 had the highest homology to the human MUC20 cDNA. By a PCR screen employing the sequences of these ESTs, we isolated a mouse cognate from a mouse kidney cDNA library. Fig. 1*A* shows the amino acid sequence alignment of the proteins encoded by the human and mouse clones. The predicted sequence of mouse MUC20, consisting of 656 amino acids, shows similar characteristics to human MUC20, such as bearing several hydrophobic domains and three mucin repeats of 18 amino acids in its N-terminal region. The sequences are most similar in the C-terminal domain (48% identity overall and 62% identity in the C-terminal 50 amino acids) but less similar in the N-terminal portions. Interestingly, the position and sequence of the mucin tandem domain of mouse MUC20 do not coincide with those of human MUC20, although the predominance of threonines, serines, and prolines in this domain is conserved.

Genomic Structure and Alternative Transcription of Human MUC20—Next, we characterized the genomic structure of human *MUC20*. By screening ~1.0 $\times$ 10^6 plaques of a human genomic library with the human MUC20 coding region, we obtained 24 positive clones. Analysis of the genomic fragments revealed that the isolated human MUC20 cDNA was derived from three exons. Significantly, the genomic DNA clone encoded 6 repeats of the tandem sequence in the mucin domain (data not shown), whereas the cDNA clone encoded only three.

An EST clone (GenBank™/EBI Data Bank accession number AK027314), which was isolated from a human 10-week whole embryo cDNA library, showed significant identity with the human MUC20 cDNA. Comparison of the AK027314 protein with human MUC20 revealed an additional hydrophobic peptide of 35 amino acids at the N terminus of AK027314 (Fig. 2*A*). Therefore, we termed the AK027314 type of human MUC20 as hMUC20-L and the shorter one encoded by our cDNA clone as hMUC20-S. We searched the NCBI data base for the exon encoding the additional N-terminal peptide of hMUC20-L. The exon was found ~3.6 kbp upstream from the *exon-2* of the *MUC20* gene (Fig. 2, *A* and *B*). These results raised the possibility of alternative promoters that gave rise to the different forms of the human MUC20 mRNA. To rule out

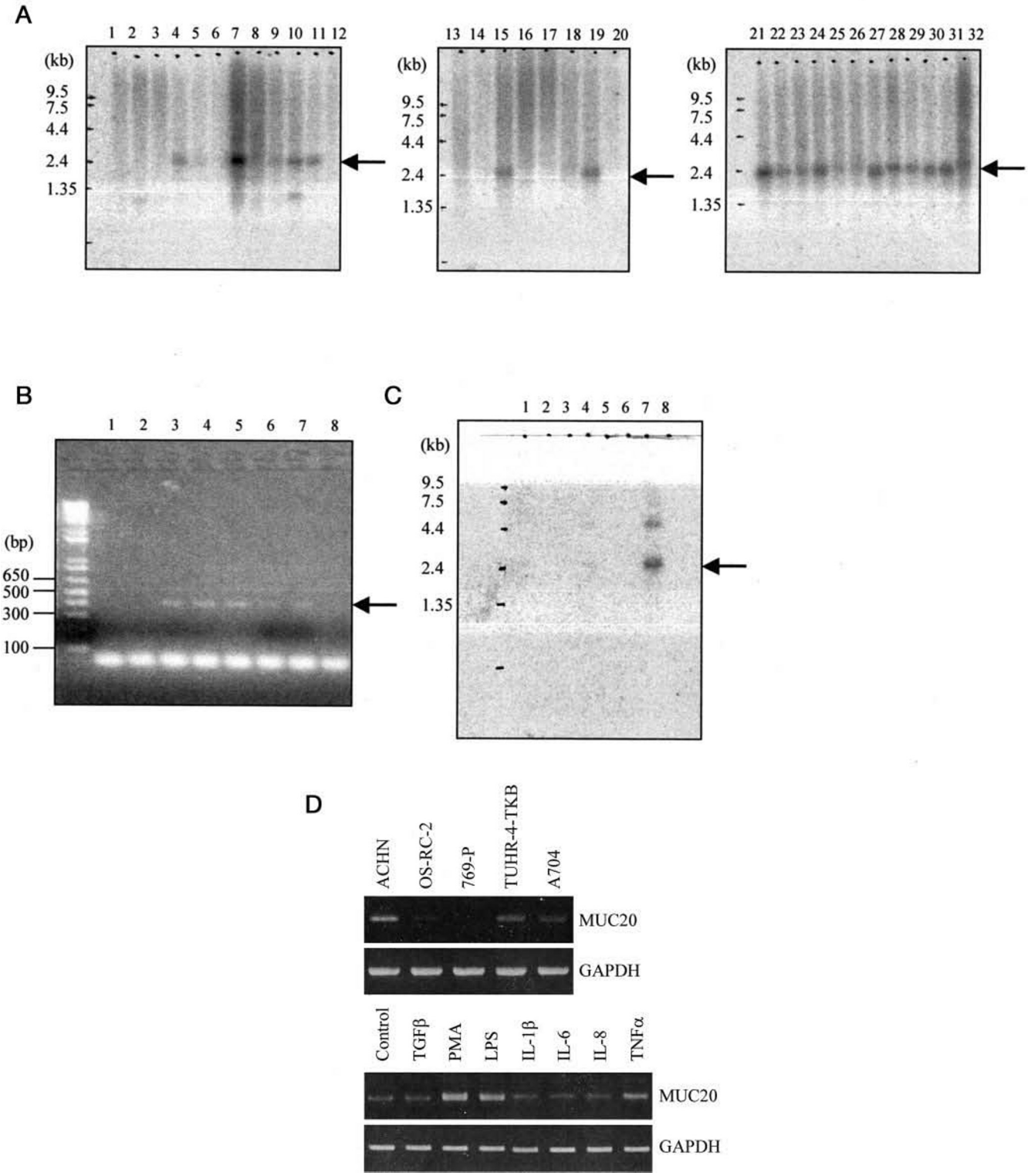

FIG. 4. **Expression of MUC20 in various tissues and cell lines.** *A*, Northern blot analysis of MUC20 mRNA in various human tissues. The *exon-4* segment of human *MUC20* was used as a probe. The molecular sizes (in kb) are shown on the *left*. The *arrow* on the *right* indicates MUC20 mRNAs. *Lane 1*, brain; *lane 2*, heart; *lane 3*, muscle; *lane 4*, colon; *lane 5*, thymus; *lane 6*, spleen; *lane 7*, kidney; *lane 8*, liver; *lane 9*, small intestine; *lane 10*, placenta; *lane 11*, lung; *lane 12*, peripheral blood leukocyte; *lane 13*, spleen; *lane 14*, thymus; *lane 15*, prostate; *lane 16*, testis; *lane 17*, ovary; *lane 18*, small intestine; *lane 19*, colon; *lane 20*, peripheral blood leukocyte; *lane 21*, esophagus; *lane 22*, stomach; *lane 23*, duodenum; *lane 24*, ileocecum; *lane 25*, ileum; *lane 26*, jejunum; *lane 27*, ascending colon; *lane 28*, descending colon; *lane 29*, transverse colon; *lane 30*, cecum; *lane 31*, rectum; *lane 32*, liver. *B*, expression analysis of MUC20 mRNA in human tissues by RT-PCR of the *exon-2* and *exon-3* region. *Lane 1*, brain; *lane 2*, heart; *lane 3*, kidney; *lane 4*, liver; *lane 5*, lung; *lane 6*, pancreas; *lane 7*, placenta; *lane 8*, skeletal muscle. The *arrow* on the *right* indicates amplified DNAs representing the MUC20 mRNA. *C*, Northern blot analysis of MUC20 mRNA in mouse tissues. The *exon-2* segment of mouse *MUC20* was used as a probe. *Lane 1*, heart; *lane 2*, brain; *lane 3*, spleen; *lane 4*, lung; *lane 5*, liver; *lane 6*, muscle; *lane 7*, kidney; *lane 8*, testis. The *arrow* on the *right* indicates MUC20 mRNAs. *D*, RT-PCR analysis of MUC20 expression in several human kidney cell lines. *Upper*, in ACHN, OS-RC-2, 769-P, TUHR-4-TKB, and A704 cells. *Lower*, in ACHN cells stimulated with transforming growth factor-β (*TGF*β, 2 ng/ml), phorbol 12-myristate 13-acetate (*PMA*, 100 μM), lipopolysaccharide (*LPS*, 10 μg/ml), IL-1β (0.4 ng/ml), IL-6 (100 ng/ml), IL-8 (250 ng/ml), or tumor necrosis factor-α (*TNF*α, 100 ng/ml) for 14 h. The expression of GAPDH mRNA is shown as a control for each sample.

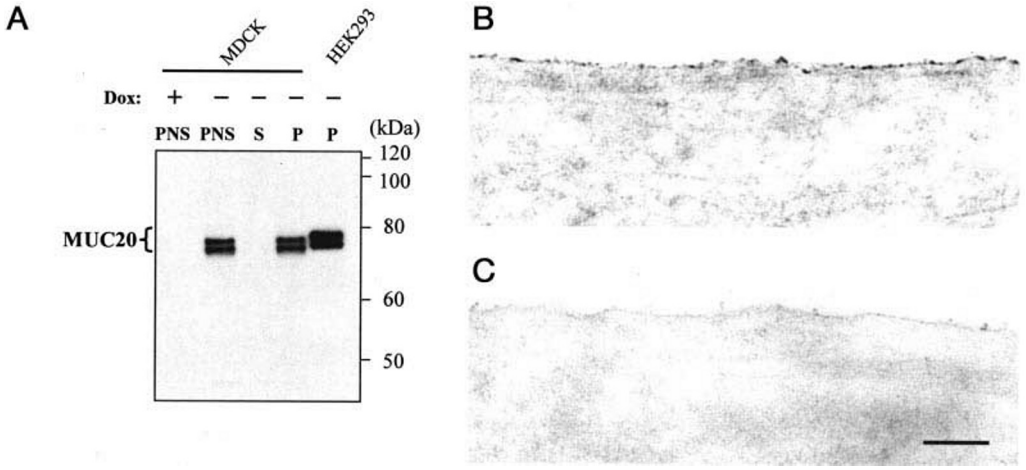

FIG. 5. **Localization of MUC20 protein.** *A*, immunoblot analysis of human MUC20 produced in MDCK/*tet*-MUC20 and HEK293/*tet*-MUC20 cells, using anti-MUC20 polyclonal antibody. Cells were cultured in the absence of Dox (−) to induce production of MUC20 or in the presence of Dox (+) as a control. *PNS*, postnuclear supernatant; *S*, cytosolic 100,000 × *g* supernatant; *P*, the 100,000 × *g* membrane pellet fraction. *B* and *C*, immunoelectron microscopic analysis of human MUC20-producing MDCK/*tet*-MUC20 cells by preembedding immunoperoxidase staining. Immunoreactivity with the anti-MUC20 polyclonal antibody was localized on the plasma membrane. There was no apparent staining in the cytoplasm (*B*). No staining was seen with control rabbit IgG (*C*). *Bar*, 250 nm.

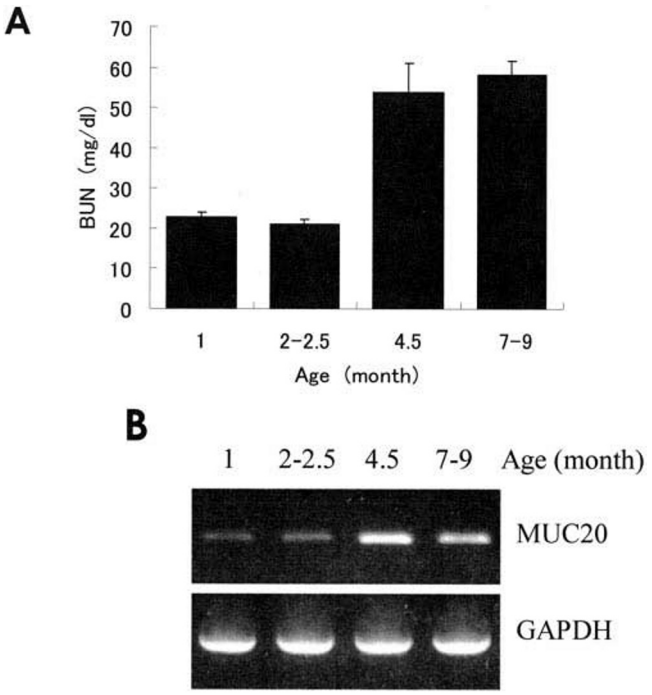

FIG. 6. **MUC20 mRNA in renal tissues of *MRL/MpJ-lpr/lpr* mice with the progression of lupus nephritis.** *A*, levels of BUN, reflecting progression of renal injury in *MRL/MpJ-lpr/lpr* mice with age (1 month old (n = 20), 2–2.5 months old (n = 13), 4.5 months old (n = 12), and 7–9 months old (n = 15), mean ± S.E.). *B*, MUC20 mRNA in renal tissue of MRL/MpJ-*lpr/lpr* mice during the development of renal injury. Equal amounts of total RNA were prepared from the renal tissues of the same mice used to measure BUN in *A* and were mixed together and used as PCR templates. RT-PCR products representing MUC20 mRNA and GAPDH mRNA are shown in the *upper* and *lower panels*, respectively.

the possibility that the hMUC20-S cDNA was produced from an immature mRNA containing unspliced introns, we performed 5′-rapid amplification of cDNA ends (5′-RACE) on MUC20 mRNA from human kidney using three sets of primers. As shown in Fig. 2*C*, each set of primers amplified a single species of DNA, and sequence analysis revealed that each of these DNAs had the same 5′-end as the hMUC20-S cDNA. These results indicate that at least two transcriptional start points exist in the *hMUC20* gene, encoding two isoforms of the hMUC20 protein with different N-terminal sequences. These results also suggest that hMUC20-S is expressed highly in human kidney, whereas hMUC20-L was not detected in these experimental conditions, although it was isolated from human 10-week-old whole embryo. Interestingly, the sequence of the N-terminal peptide of hMUC20-L shows high identity to that of mouse MUC20, indicating that the isolated mouse MUC20 could be the counterpart of the hMUC20-L form (Fig. 2*A*).

Comparison of our cloned human *MUC20* gene fragments with the working draft version of the human genome sequences available from NCBI showed that they are included in fragment AC025282, localized on chromosome 3q29. We also found that the *MUC4* gene is located very close to *MUC20*, supporting the existence of a cluster domain of transmembrane mucin genes at this locus. Surprisingly, sequencing and Southern blot analyses of our cloned genomic fragments revealed that these clones fell into two groups. One group of clones contained sequences from *exon-1* to *exon-4* of the *hMUC20* gene, whereas the other group had a segment 98% identical to *exon-1*, *intron-1*, and *exon-2* followed by sequences showing no similarity to the *intron-2* and lacking both the *exon-3* and *exon-4* regions (Fig. 2*D*). This second group was named the *MUC20-like* segment. Southern blot analysis of human genomic DNA revealed two restriction fragments from EcoRI, HindIII, or BamHI digests when probed with an *exon-2* fragment; however, a single band was detected using an *exon-4* probe (Fig. 2*E*). Searching the NCBI data base also revealed the existence of a locus similar to *MUC20*, completely matching the *MUC20-like* segment sequence, located ~200 kbp downstream of the *MUC20* gene (Fig. 2*D*). It is not yet clear whether this *MUC20-like* locus is transcribed, and searching for tissues or cells that express this gene is underway in our laboratory. In contrast, Southern blot analysis of mouse genomic DNAs revealed the presence of single EcoRI-, EcoRV-, or HindIII-digested fragments using the *exon-2* region of the mouse *MUC20* gene as a probe (Fig. 2*F*). The genomic structure of the mouse *MUC20* gene, located on mouse chromosome 16, is, however, very similar to that of the human *MUC20* gene, *e.g.* comprising four exons (data not shown).

Polymorphism of the Mucin Tandem Domain—As mentioned above, the repeat numbers of the tandem domain in human MUC20 showed a divergence, with 3 repeats in the cDNA clone and 6 repeats in the genomic clone. These findings prompted us to examine polymorphism of this domain. Sequencing of human

MUC20 cDNAs and genomic DNAs isolated from other libraries revealed the existence of 2-, 4-, and 5-repeat types of human MUC20 (Fig. 3*A*). To further investigate the variation of the repeat numbers in this domain, the polymorphic regions of human *MUC20* in genomic DNAs from several human cell lines were amplified by PCR, and the repeat numbers were estimated from the length of the amplified DNA fragments. The primers could anneal to sequences in the *MUC20-like* locus as well as *MUC20*, resulting in 1–4 bands for each cell line. As shown in Fig. 3*B*, the amplified DNA fragments corresponded to 2-, 3-, 4-, 5-, or 6-repeat lengths. Taken together, these results indicate polymorphism in the mucin tandem domain of the human *MUC20* gene.

Expression of MUC20 in Human and Mouse Tissues—To examine the expression of MUC20, poly(A)+ RNA from various human tissues was subjected to Northern blot and RT-PCR analyses (Fig. 4, *A* and *B*). MUC20 mRNA (~2.5 kb) was abundantly detected in kidney and moderately in placenta, lung, prostate, liver, and digestive system (*e.g.* colon, esophagus, and rectum) using the *exon-4* segment of human *MUC20* as a probe. No difference in the distribution of MUC20 mRNA was obtained by using the *exon-2* probe, which has 98% identity to the corresponding region in the *MUC20-like* segment, suggesting that expression of *MUC20-like* mRNA may be low or absent in these tissues (data not shown). Likewise, mouse MUC20 mRNA (~2.5 kb) was highly expressed in kidney (Fig. 4*C*). Normal human kidney was immunohistochemically stained using a polyclonal antibody to the N-terminal region of human MUC20. Antibody to aquaporin-1, a marker for proximal tubules, was used to identify the types of epithelium in the serial section. The results indicate that MUC20 protein is localized in the proximal tubules but not in the glomerulus or distal tubules (supplemental data). Several cell lines established from human kidney, ACHN, TUHR-4-TKB, and A704 cells, were found to express easily detectable levels of MUC20 mRNA (Fig. 4*D*). One of these cell lines, ACHN, which is known as a renal tubular epithelial line established from malignant pleural effusion of a patient with metastatic renal adenocarcinoma (32), was used to examine transcriptional regulation in response to various stimuli. As shown in Fig. 4*D*, stimulation with phorbol 12-myristate 13-acetate, lipopolysaccharide, or tumor necrosis factor-α, but not transforming growth factor-β, IL-1β, IL-6, or IL-8, significantly increased MUC20 mRNA expression in this cell line.

Localization of MUC20 Protein—To test the subcellular localization of MUC20 protein, we prepared human MUC20-producing cells, MDCK/*tet*-MUC20 cells, and HEK293/*tet*-MUC20 cells from MDCK and HEK293 cells. These cells express C-terminally FLAG-tagged human MUC20 under control of a *tet* promoter, and the production of MUC20 protein was strongly enhanced by reduction of Dox in the culture medium. The cells were fractionated, and the fractions were subjected to immunoblotting using the anti-MUC20 polyclonal antibody. In MDCK/*tet*-MUC20 cells, two bands of ~76 and 78 kDa, which were not detected under the suppressing condition, were observed in the membrane-rich fraction under the inducing condition (Fig. 5*A*). The same results were obtained with anti-FLAG antibody (data not shown). Interestingly, the mobility of these proteins on SDS-PAGE was slightly different from that of the proteins from HEK293/*tet*-MUC20 cells (~77 and 79 kDa) (Fig. 5*A*). Immunoelectron microscopy with anti-MUC20 antibody demonstrated MUC20 immunoreactivity on the plasma membrane of the MUC20-producing MDCK/*tet*-MUC20 cells (Fig. 5*B*), whereas the cells reacted with control rabbit IgG did not show such staining (Fig. 5*C*). MDCK/*tet*-MUC20 cells cultured in the presence of Dox did not show the staining with either the anti-MUC20 antibody or control rabbit IgG (data not shown).

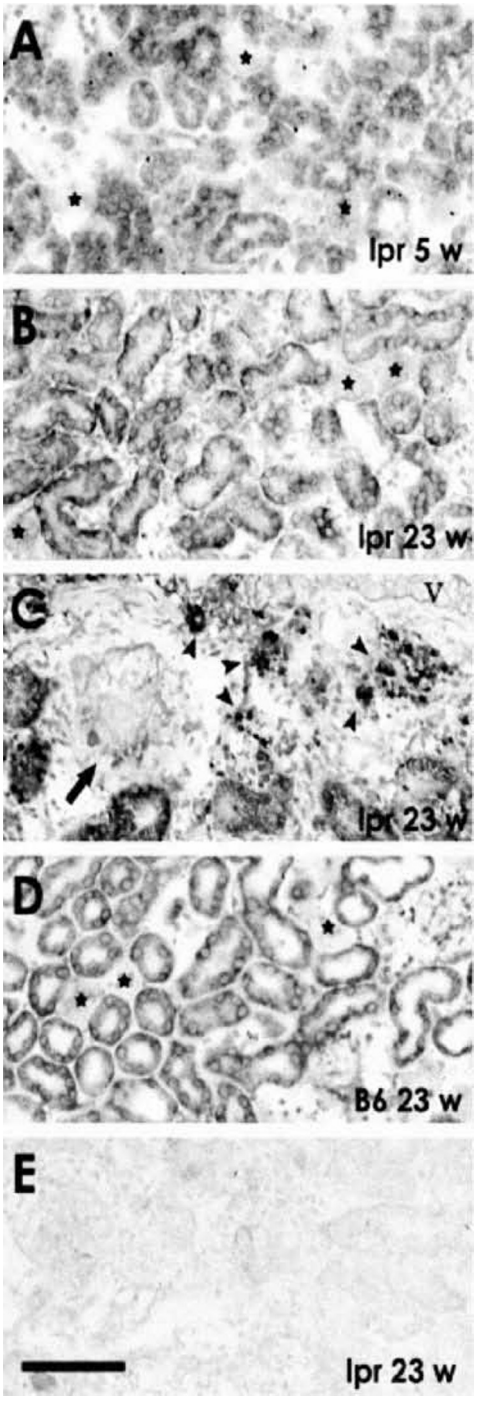

FIG. 7. ***In situ* hybridization analysis of kidney sections from MRL/MpJ-*lpr/lpr* mice and normal mice.** Kidney sections were subjected to *in situ* hybridization with digoxigenin-labeled *MUC20* cRNA probe fragment 7-11 (892 bp, C-terminal domain). In *A*, 5-week-old MRL/MpJ-*lpr/lpr* mice, the proximal tubules showed signal for MUC20 mRNA, whereas the distal tubules (*stars*) showed no signal. In *B*, when mice were 23 weeks old, the signals were significantly increased in the proximal tubules, but not the distal tubules (*stars*), of MRL/MpJ-*lpr/lpr* mice. *C*, at this age, pathological changes including glomerular lesion (*arrow*) and arteritis become prominent, and a certain population of inflammatory interstitial cells in the vicinity of an artery (*v*) also expressed the mRNA (*arrowheads*). In *D*, control tissues of 23-week-old C57Bl(B6) mice showed MUC20 mRNA in the proximal tubules but not in the distal tubules (*stars*). In *E*, the 23-week-old MRL/MpJ-*lpr/lpr* mice showed no signal with sense probe. *Bar*, 100 μm.

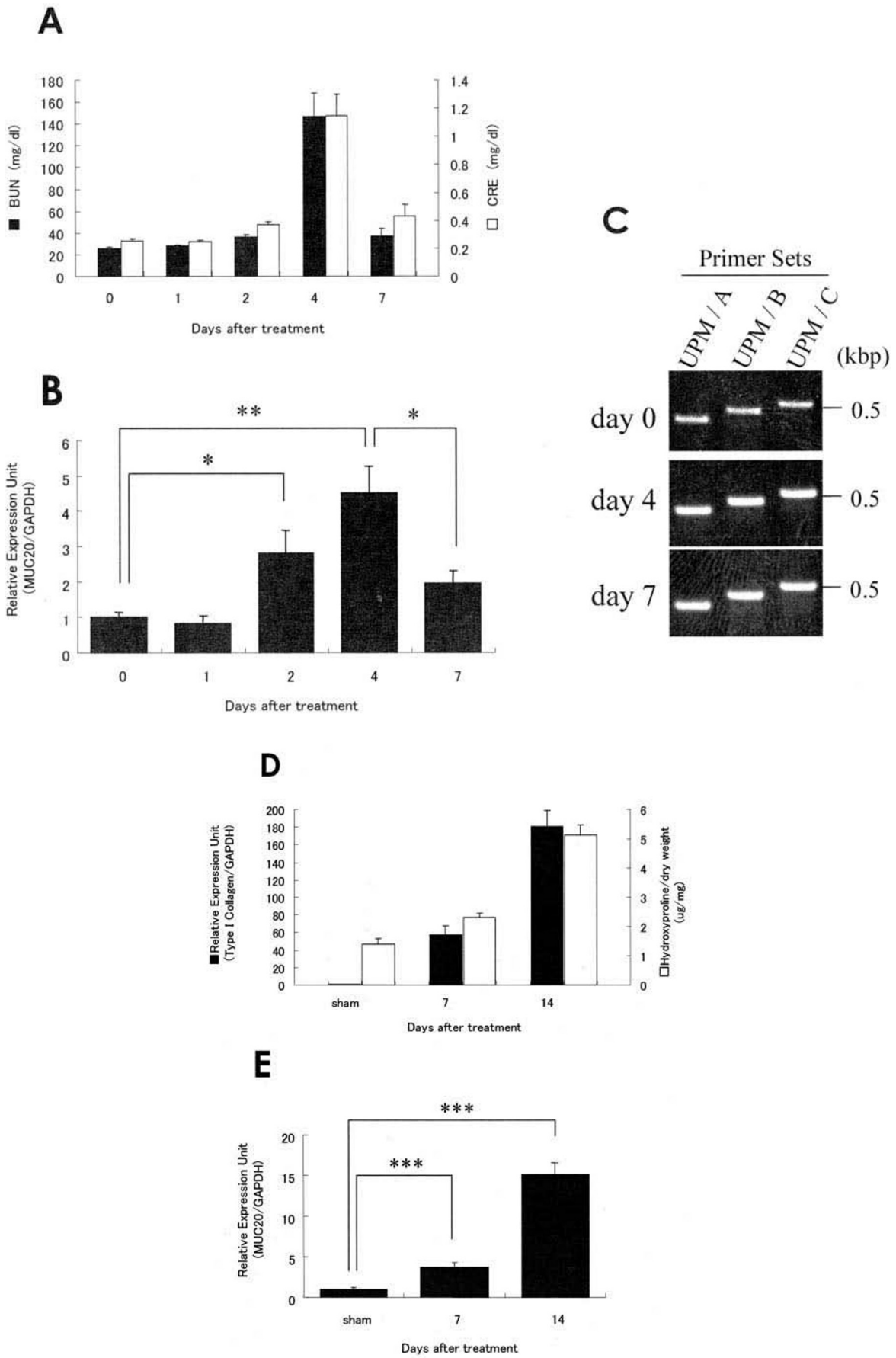

FIG. 8. **Up-regulation of MUC20 mRNA expression during acute renal failure.** In *A* and *B*, changes of MUC20 mRNA expression in ICR mice with acute renal failure caused by cisplatin administration. Results are from one of two independent experiments. Renal damage was determined by measuring both serum creatinine (*CRE*) and BUN ($n = 5$, mean ± S.E.) (*A*). Levels of MUC20 mRNA in the renal tissues of mice

Up-regulation of Mouse MUC20 mRNA in Injured Kidneys—To determine whether the expression of MUC20 mRNA changes during progression of renal injury in an animal model, the levels of MUC20 mRNA were examined in the MRL/MpJ-*lpr/lpr* mouse, which is a well known model for human lupus nephritis (33, 34). MRL/MpJ-*lpr/lpr* mice were sacrificed at various ages, and renal injury was monitored by the increase in BUN, which is a parameter for evaluation of a renal damage (Fig. 6*A*). RT-PCR assays showed that, in parallel with the increase in BUN, MUC20 mRNA expression increased in the renal tissues during progression of the injury (Fig. 6*B*).

To define histologically the types of cells that express MUC20 mRNA and the change in its expression, *in situ* hybridization analysis was performed on kidney sections from MRL/MpJ-*lpr/lpr* mice using DIG-labeled MUC20 cRNA probes. As a positive control, we also carried out the *in situ* hybridization using a cRNA probe for the TSC-22 mRNA, which has been shown to localize in the proximal tubules (35) (data not shown). Two cRNA probes, fragment 5-1 (747 bp) and fragment 7-11 (892 bp), gave the same pattern of MUC20 mRNA localization. Here we show the results with fragment 7-11. In 5-week-old MRL/MpJ-*lpr/lpr* mice with no apparent renal damage, MUC20 mRNA was detected in the cytoplasm of epithelial cells constituting the proximal tubules but not in those of the distal tubules (Fig. 7*A*), and approximately the same was observed in 23-week-old C57Bl(B6) control mice (Fig. 7*D*). In contrast, in 23-week-old MRL/MpJ-*lpr/lpr* mice showing prominent lesions in the glomerulus, signals in the cells of proximal tubules were significantly augmented (Fig. 7*B*). Likewise, we observed progressive increases in MUC20 mRNA expression in MRL/MpJ-*lpr/lpr* mice from 9 to 60 weeks old (data not shown). In older MRL/MpJ-*lpr/lpr* mice with arteritis, a certain population of inflammatory cells showed significant signal with the MUC20 cRNA probes (Fig. 7*C*). The renal section from 23-week-old MRL/MpJ-*lpr/lpr* mice did not show labeling with a probe complementary to antisense RNA (Fig. 7*E*).

To further clarify the expression of MUC20 mRNA in renal disease, we used murine models in which acute renal failure is induced by administration of cisplatin, widely used as an antitumor drug, or by UUO. The amounts of MUC20 mRNA were examined by quantitative RT-PCR at multiple time points following treatment. In the cisplatin model, renal damage in each mouse was determined by measuring both serum creatinine and BUN. Both serum parameters increased until day 4 after treatment, and then returned to baseline within 7 days, as reported previously (36) (Fig. 8*A*). In this model, a parallel ~5-fold increase in MUC20 expression was observed during renal damage progression (Fig. 8*B*). To determine whether different variants of the transcripts are generated during acute renal failure, we further analyzed the MUC20 mRNA by 5′-RACE PCR using kidney RNA from day-0, day-4, and day-7 mice. The results, shown in Fig. 8*C*, revealed a single species of MUC20 mRNA, equivalent to hMUC20-L, in the day-0 mice, and no other variants were detected during the progression of cisplatin-induced renal failure. In the UUO model mice, renal injury and fibrosis were estimated by the changes in collagen type I mRNA levels and hydroxyproline content in the kidney. Marked increases in both hydroxyproline content and type I collagen mRNA levels were observed at day 7 and day 14 following UUO (Fig. 8*D*), and the level of MUC20 mRNA increased in parallel (Fig. 8*E*).

DISCUSSION

We report here the molecular cloning, gene structure, expression, and cellular localization analyses of MUC20, a novel mucin protein, which is up-regulated in renal tissues during renal injury. To date, mucin gene clusters have been found on human chromosomes 11p15.5 and 7q22. In this report, human chromosome 3q29 was shown to contain another cluster of mucin genes, *MUC4, MUC20*, and the *MUC20-like* segment. Additionally, at least two variants (hMUC20-L and hMUC20-S) are produced from the human *MUC20* gene by alternative transcription, although only one of the corresponding variants has been so far identified in mouse tissues.

Immunoblotting analysis of human MUC20 produced in MDCK/*tet*-MUC20 cells showed MUC20 in the membrane fraction. Immunoelectron microscopic analysis of human MUC20 protein produced in MDCK/*tet*-MUC20 cells demonstrated that the immunoreactive site of anti-MUC20 antibody to N-terminal peptide was on the plasma membrane. Thus, human MUC20 protein is a membrane protein localized on the plasma membrane. We found slightly different molecular masses for MUC20 protein in MDCK/*tet*-MUC20 and HEK293/*tet*-MUC20 cells (~76~79 kDa). Since the predicted molecular mass of human MUC20 (503 amino acids) is ~55 kDa, the difference of the molecular mass might be due to posttranslational modifications (*e.g. O*-glycosylation on Ser/Thr residues). The additional peptide at the N terminus of hMUC20-L is likely a signal peptide. Since the S-form, which has no signal peptide at the N-terminal region, is localized on the plasma membrane, the L-form might be a secreted type; this hypothesis will be examined by subcellular localization analysis in the near future.

Northern blot and RT-PCR analyses demonstrated that the mRNAs of human and mouse MUC20 are predominantly expressed in the kidney. Immunohistochemical analysis of normal human kidney and *in situ* hybridization analysis of renal sections from MRL/MpJ-*lpr/lpr* and normal mice revealed that MUC20 is produced in the epithelium of proximal tubules but not in that of distal tubules. The intensity of the signals progressively increased during the development of glomerulonephritis in MRL/MpJ-*lpr/lpr* mice. Although the other organs were well fixed by cardiac perfusion, kidneys of 23- and 60-week-old MRL/MpJ-*lpr/lpr* mice resisted fixation. This difficulty of the fixation by perfusion suggests that there were glomerular lesions in these kidneys. This analysis also showed MUC20 expression in a certain population of interstitial inflammatory cells in the sites of arteritis, which is a pathological characteristic of MRL/MpJ-*lpr/lpr* mice (37). Interstitial inflammatory cell infiltrate usually consists of plasma cells, lymphocytes, and polymorphonuclear leukocytes, but it remains to be investigated which cell type or types express MUC20 mRNA and what role MUC20 plays in these cells. Taken together, these results suggest that the expression of MUC20 mRNA in

at each stage were determined by quantitative RT-PCR. No significant differences were observed in GAPDH mRNA expression among these samples (data not shown); therefore, the results are represented as an average of the ratio of MUC20 mRNA levels to GAPDH mRNA levels, mean ± S.E. (*B*). *C*, RACE PCR analysis of the 5′-terminus of MUC20 mRNA in the ICR mice with acute renal failure caused by cisplatin administration. These experiments used total RNA and the primer sets depicted in Fig. 2*B*. The primer sets used in each reaction are indicated *above* the *lanes*. *UPM*, Universal Primer Mix™ (Clontech). *D* and *E*, augmentation of MUC20 mRNA expression in C57Bl(B6) mice after UUO. Results are from one of two independent experiments. Hydroxyproline content in the kidney was measured on day 7 and day 14 after UUO and on day 7 after sham operation (*D*). Levels of type I collagen, MUC20, and GAPDH mRNAs were determined for each time point by quantitative RT-PCR. Since no significant changes of the GAPDH mRNA expression were observed during the development of acute renal failure (data not shown), the levels of type I collagen mRNA (*D*) and MUC20 mRNA (*E*) are represented as an average of the ratio to GAPDH mRNA levels, mean ± S.E. ($n = 6$). A two-tailed Student's t test was used for statistical analysis. *, $p < 0.05$; **, $p < 0.01$; ***, $p < 0.001$.

renal tissues, especially the epithelial cells of the proximal tubules, was enhanced with the progression of lupus nephritis. Progressive increases in MUC20 expression in these models suggest that MUC20 might play an important role in glomerulonephritis.

In normal human kidney, MUC1 mRNA localizes to the distal convoluted tubules, Henle's loops, and collecting ducts, whereas the expression of MUC3 and KIM-1 mRNAs is restricted to the proximal tubules (3, 4). Expression of MUC3 and KIM-1 mRNAs is up-regulated in renal cell carcinoma patients and postischemic rat kidney, respectively (3, 4). MUC1 expression levels have been inversely correlated with postsurgical survival of patients with renal cell carcinoma (38). Recently, we have found that human MUC20 mRNA was up-regulated in renal tissues of patients with moderate IgAN as compared with the mild stage IgAN or normal tissues, although these increases were not observed in IgAN renal tissues of patients with severe damage (24). The decreased expression of MUC20 mRNA in the severely injured tissues as compared with those of the moderate stage might be due to significant damage in the epithelial cells of proximal tubules because it has been reported that the epithelial cells of proximal and distal tubules are remarkably impaired in the heavily damaged renal tissues of IgAN patients (39).

In this work, we also demonstrated divergence in repeat numbers of the mucin tandem domain (2–6 repeats) in human MUC20 by the analysis of the several MUC20 clones (cDNAs and genomic DNAs) from different human libraries. Most of the mucin genes had an extensive tandem repeat domain, but this domain showed allelic differences in length. The variation of the repeat numbers will affect not only the amount of glycosylation but also probably other physicochemical properties. Both effects may have functional consequences and lead to differences in disease susceptibility. It has been reported that individuals with small numbers of tandem repeats in MUC1 have an increased risk of gastric carcinoma (40). Associations between allelic variants of MUC2 (41) and MUC7 (42) and atopy with or without asthma have also been reported. Together with these previous reports, our finding that MUC20 expression is increased in IgAN patients and animal models of renal injury suggests that the repeat numbers of the MUC20 mucin domain might be implicated in the pathogenesis of renal diseases.

Epithelial mucins are thought to function in cell protection, adhesion modulation, and signaling. A recent report has shown that cell adhesion of *Pseudomonas aeruginosa*, a Gram-negative bacterium, was enhanced by the presence of MUC1 on the cell surface (43). MUC7 has been shown to interact with a variety of bacteria including four strains of *Streptococci* (44), *Actinobacillus actinomycetemcomitans* (45), *Staphylococcus aureus*, and *P. aeruginosa* (46), and it may have a role in facilitating the clearance of oral bacteria. Moreover, two sulfate mucin-type glycoproteins on lymph node endothelium were found to bind lymphocyte L-selectin (47, 48), whereas sialylated and fucosylated mucin-types were shown to bind P-selectin (49, 50). In addition, the mucin region of mucosal addressing cell adhesion molecule-1 (MAdCAM-1) can bind L-selectin (51). Therefore, we suggest that the extracellular mucin portion of MUC20 might interact with bacteria or with distinct cellular ligands, such as selectins, and play a pivotal role in protective functions or cell adhesion. At present, our laboratory is investigating which molecules recognize the extracellular portion of MUC20. Several mucins are known to have cell signaling roles; such a role is particularly well documented for MUC1. Recent studies have demonstrated that tyrosine phosphorylation of the MUC1 cytoplasmic domain correlates with changes in cell-cell adhesion (52). Ligand-activated epidermal growth factor receptor interacts with MUC1 and enhances the phosphorylation of its cytoplasmic domain, leading to recruitment of signaling molecules, such as Grb2, son of sevenless, c-Src, and β-catenin, to MUC1 (53). This also induces activation of extracellular signal-regulated kinases 1/2 (ERK1/2), suggesting that MUC1 regulates cell growth and differentiation through the Grb2/SOS/Ras/ERK signaling cascade (54–56). Moreover, it appears that the cytoplasmic domain of MUC1 associates with cell adhesion molecules β- and γ-catenins (57), and the serine phosphorylation of the cytoplasmic domain by glycogen synthase kinase 3β decreases binding of MUC1 to β-catenin (58). These findings suggest that cell signaling is a plausible role for MUC20. It is also suggestive that the amino acid sequences of human and mouse MUC20 showed 48% identity in the C-terminal domain, with especially strong homology (62%) in the C-terminal 50 amino acids but less similarity in the other portions. This high conservation across mammalian species suggests that this region might play a crucial role in MUC20 function. Functional analyses of the cytoplasmic tail of MUC20 are underway in our laboratory.

In summary, we have identified the complete cDNA sequence for a novel mucin membrane protein, MUC20, which is expressed in human and mice proximal tubules and markedly up-regulated during renal injury. Further characterization of MUC20 and related molecules will elucidate the role of MUC20 protein in the development and progression of several renal diseases.

Acknowledgments—We thank Drs. M. Sasabuchi, K. Akiyama, J. Yamamoto, H. Sasai, K. Iwata, T. Chuman (Japan Tobacco Central Pharmaceutical Frontier Research Laboratories), and Dr. E. Imai (Osaka University) for fruitful discussion, and we thank M. Tanaka and M. Ohnishi (Japan Tobacco Central Pharmaceutical Research Institute) for *in vivo* experiments. We also thank the staff of Japan Tobacco Creative Service, H. Murakoshi, I. Suganuma, K. Ishii, M. Saito, S. Kubo, Y. Mohara, and N. Ookawara, for technical assistance.

REFERENCES

1. Thadhani, R., Pascual, M., and Bonventre, J. V. (1996) *N. Engl. J. Med.* **334,** 1448–1460
2. Sheridan, A. M., and Bonventre, J. V. (2000) *Curr. Opin. Nephrol. Hypertens.* **9,** 427–434
3. Leroy, X., Copin, M. C., Devisme, L., Buisine, M. P., Aubert, J. P., Gosselin, B., and Porchet, N. (2002) *Histopathology* **40,** 450–457
4. Ichimura, T., Bonventre, J. V., Bailly, V., Wei, H., Hession, C. A., Cate, R. L., and Sanicola, M. (1998) *J. Biol. Chem.* **273,** 4135–4142
5. Gum, J. R., Jr., Hicks, J. W., Toribara, N. W., Siddiki, B., and Kim, Y. S. (1994) *J. Biol. Chem.* **269,** 2440–2446
6. Guyonnet-Duperat, V., Audie, J. P., Debailleul, V., Laine, A., Buisine, M. P., Galiegue-Zouitina, S., Pigny, P., Degand, P., Aubert, J. P., and Porchet, N. (1995) *Biochem. J.* **305,** 211–219
7. Desseyn, J. L., Guyonnet-Duperat, V., Porchet, N., Aubert, J. P., and Laine, A. (1997) *J. Biol. Chem.* **272,** 3168–3178
8. Toribara, N. W., Roberton, A. M., Ho, S. B., Kuo, W. L., Gum, E., Hicks, J. W., Gum, J. R., Jr., Byrd, J. C., Siddiki, B., and Kim, Y. S. (1993) *J. Biol. Chem.* **268,** 5879–5885
9. Bobek, L. A., Tsai, H., Biesbrock, A. R., and Levine, M. J. (1993) *J. Biol. Chem.* **268,** 20563–20569
10. Shankar, V., Gilmore, M. S., Elkins, R. C., and Sachdev, G. P. (1994) *Biochem. J.* **300,** 295–298
11. Arias, E. B., Verhage, H. G., and Jaffe, R. C. (1994) *Biol. Reprod.* **51,** 685–694
12. Gendler, S. J., Lancaster, C. A., Taylor-Papadimitriou, J., Duhig, T., Peat, N., Burchell, J., Pemberton, L., Lalani, E. N., and Wilson, D. (1990) *J. Biol. Chem.* **265,** 15286–15293
13. Lan, M. S., Batra, S. K., Qi, W. N., Metzgar, R. S., and Hollingsworth, M. A. (1990) *J. Biol. Chem.* **265,** 15294–15299
14. Williams, S. J., Munster, D. J., Quin, R. J., Gotley, D. C., and McGuckin, M. A. (1999) *Biochem. Biophys. Res. Commun.* **261,** 83–89
15. Moniaux, N., Nollet, S., Porchet, N., Degand, P., Laine, A., and Aubert, J. P. (1999) *Biochem. J.* **338,** 325–333
16. Williams, S. J., McGuckin, M. A., Gotley, D. C., Eyre, H. J., Sutherland, G. R., and Antalis, T. M. (1999) *Cancer Res.* **59,** 4083–4089
17. Williams, S. J., Wreschner, D. H., Tran, M., Eyre, H. J., Sutherland, G. R., and McGuckin, M. A. (2001) *J. Biol. Chem.* **276,** 18327–18336
18. Pallesen, L. T., Berglund, L., Rasmussen, L. K., Petersen, T. E., and Rasmussen, J. T. (2002) *Eur. J. Biochem.* **269,** 2755–2763
19. Yin, B. W., and Lloyd, K. O. (2001) *J. Biol. Chem.* **276,** 27371–27375
20. Gum, J. R., Jr., Crawley, S. C., Hicks, J. W., Szymkowski, D. E., and Kim, Y. S. (2002) *Biochem. Biophys. Res. Commun.* **291,** 466–475
21. Lehmann, J. M., Riethmuller, G., and Johnson, J. P. (1989) *Proc. Natl. Acad. Sci. U. S. A.* **86,** 9891–9895

22. Pigny, P., Guyonnet-Duperat, V., Hill, A. S., Pratt, W. S., Galiegue-Zouitina, S., d'Hooge, M. C., Laine, A., Van-Seuningen, I., Degand, P., Gum, J. R., Kim, Y. S., Swallow, D. M., Aubert, J. P., and Porchet, N. (1996) *Genomics* **38,** 340–352
23. Prashar, Y., and Weissman, S. M. (1999) *Methods Enzymol.* **303,** 258–272
24. Waga I., Yamamoto J., Sasai H., Munger, W. E., Hogan S., Preston, G. A., Jennette, J. C., Falk, R. J., and Alcorta, D. A. (2003) *Kidney Int.* **64,** 1253–1264
25. Sambrook, J., Fritsch, E. F., and Maniatis, T. (1985) *Molecular Cloning: A Laboratory Manual*, pp. 8.3–8.82, Cold Spring Harbor Laboratory Press, Cold Spring Harbor, NY
26. Nakamura, M., Watanabe, H., Kubo, Y., Yokoyama, M., Matsumoto, T., Sasai, H., and Nishi, Y. (1998) *Recept. Channels* **5,** 255–271
27. Aldridge, J., Kunkel, L., Bruns, G., Tantravahi, U., Lalande, M., Brewster, T., Moreau, E., Wilson, M., Bromley, W., Roderick, T., and Latt, S. A. (1984) *Am. J. Hum. Genet.* **36,** 546–564
28. Yang, J., Dai, C., and Liu, Y. (2002) *J. Am. Soc. Nephrol.* **13,** 2464–2477
29. Blumenkrantz, N., and Asboe-Hansen, G. (1973) *Anal. Biochem.* **55,** 288–291
30. Boehringer Mannheim (1992) *Boehringer Mannheim Technical Bulletin, Nonradioactive in Situ Hybridization Application Manual*, Indianapolis, IN
31. Altschul, S. F., Gish, W., Miller, W., Myers, E. W., and Lipman, D. J. (1990) *J. Mol. Biol.* **215,** 403–410
32. Giard, D. J., Aaronson, S. A., Todaro, G. J., Arnstein, P., Kersey, J. H., Dosik, H., and Parks, W. P. (1973) *J. Natl. Cancer Inst.* **51,** 1417–1423
33. Theofilopoulos, A. N., and Dixon, F. J. (1985) *Adv. Immunol.* **37,** 269–390
34. Cohen, P. L., and Eisenberg, R. A. (1991) *Annu. Rev. Immunol.* **9,** 243–269
35. Dohrmann, C. E., Belaoussoff, M., and Raftery, L. A. (1999) *Mech. Dev.* **84,** 147–151
36. Kawaida, K., Matsumoto, K., Shimazu, H., and Nakamura, T. (1994) *Proc. Natl. Acad. Sci. U. S. A.* **91,** 4357–4361
37. Andrews, B. S., Eisenberg, R. A., Theofilopoulos, A. N., Izui, S., Wilson, C. B., McConahey, P. J., Murphy, E. D., Roths, J. B., and Dixon, F. J. (1978) *J. Exp. Med.* **148,** 1198–1215
38. Fujita, K., Denda, K., Yamamoto, M., Matsumoto, T., Fujime, M., and Irimura, T. (1999) *Br. J. Cancer* **80,** 301–308
39. Tashiro, K., Kodera, S., Takahashi, Y., Horikoshi, S., Shirato, I., and Tomino, Y. (1998) *Nephron* **79,** 21–27
40. Carvalho, F., Seruca, R., David, L., Amorim, A., Seixas, M., Bennett, E., Clausen, H., and Sobrinho-Simoes, M. (1997) *Glycoconj. J.* **14,** 107–111
41. Vinall, L. E., Fowler, J. C., Jones, A. L., Kirkbride, H. J., de Bolos, C., Laine, A., Porchet, N., Gum, J. R., Kim, Y. S., Moss, F. M., Mitchell, D. M., and Swallow, D. M. (2000) *Am. J. Respir. Cell Mol. Biol.* **23,** 678–686
42. Kirkbride, H. J., Bolscher, J. G., Nazmi, K., Vinall, L. E., Nash, M. W., Moss, F. M., Mitchell, D. M., and Swallow, D. M. (2001) *Eur. J. Hum. Genet.* **9,** 347–354
43. Lillehoj, E. P., Hyun, S. W., Kim, B. T., Zhang, X. G., Lee, D. I., Rowland, S., and Kim, K. C. (2001) *Am. J. Physiol.* **280,** L181–LL187
44. Liu, B., Rayment, S., Oppenheim, F. G., and Troxler, R. F. (1999) *Arch. Biochem. Biophys.* **364,** 286–293
45. Groenink, J., Ligtenberg, A. J., Veerman, E. C., Bolscher, J. G., and Nieuw, Amerongen, A. V. (1996) *Antonie Leeuwenhoek* **70,** 79–87
46. Biesbrock, A. R., Bobek, L. A., and Levine, M. J. (1997) *Glycoconj. J.* **14,** 415–422
47. Lasky, L. A., Singer, M. S., Dowbenko, D., Imai, Y., Henzel, W. J., Grimley, C., Fennie, C., Gillett, N., Watson, S. R., and Rosen, S. D. (1992) *Cell* **69,** 927–938
48. Baumheter, S., Singer, M. S., Henzel, W., Hemmerich, S., Renz, M., Rosen, S. D., and Lasky, L. A. (1993) *Science* **262,** 436–438
49. Norgard, K. E., Moore, K. L., Diaz, S., Stults, N. L., Ushiyama, S., McEver, R. P., Cummings, R. D., and Varki, A. (1993) *J. Biol. Chem.* **268,** 12764–12774
50. Sako, D., Chang, X. J., Barone, K. M., Vachino, G., White, H. M., Shaw, G., Veldman, G. M., Bean, K. M., Ahern, T. J., Furie, B., Cumming, D., and Larsen, G. R. (1993) *Cell* **75,** 1179–1186
51. Berg, E. L., McEvoy, L. M., Berlin, C., Bargatze, R. F., and Butcher, E. C. (1993) *Nature* **366,** 695–698
52. Quin, R. J., and McGuckin, M. A. (2000) *Int. J. Cancer.* **87,** 499–506
53. Li, Y., Ren, J., Yu, W., Li, Q., Kuwahara, H., Yin, L., Carraway, K. L., III, and Kufe, D. (2001) *J. Biol. Chem.* **276,** 35239–35242
54. Schroeder, J. A., Thompson, M. C., Gardner, M. M., and Gendler, S. J. (2001) *J. Biol. Chem.* **276,** 13057–13064
55. Pandey, P., Kharbanda, S., and Kufe, D. (1995) *Cancer Res.* **55,** 4000–4003
56. Meerzaman, D., Shapiro, P. S., and Kim, K. C. (2001) *Am. J. Physiol.* **281,** L86–L91
57. Yamamoto, M., Bharti, A., Li, Y., and Kufe, D. (1997) *J. Biol. Chem.* **272,** 12492–12494
58. Li, Y., Bharti, A., Chen, D., Gong, J., and Kufe, D. (1998) *Mol. Cell. Biol.* **18,** 7216–7224